Estimations of water retention curves for fine-grained soils and tailings using their fractal particle size distributions

Arturo Jimenez[1], and *Adrian* R. Russell[1]*

[1]Centre for Infrastructure Engineering and Safety, School of Civil and Environmental Engineering, The University of New South Wales, Sydney, NSW, 2052, Australia

Abstract. A water retention curve (WRC) enables the quick determination of suction in a soil or tailings using the gravimetric water content or degree of saturation. However, establishing the WRC is reliant on time consuming laboratory testing. Here an empirical method is presented that allows the WRC to be estimated quickly, including its void ratio dependency, by relating the fractal and other characteristics of the soil or tailings particle size distributions (PSD) to the parameters which define the WRC. The defining parameters, from a fractal mathematics viewpoint, depend on the particle and pore surface areas and shapes as well as their fractal dimensions. More generally, the clay percentage must also have an important role as it has a major influence on these properties, especially the surface areas. Twelve WRCs for soils and tailings were compiled and compared and used to establish the new empirical expressions. Estimated WRCs using these new empirical expressions compare well with those fitted directly to experimental results. Guidelines are also given on how to quantify suction's contribution to strength using the location of the hydraulic state on the WRC, adding to the practical appeal of this work.

1 Introduction

Water retention in soils and tailings as a function of suction is crucial in a variety of disciplines, especially engineering where assessment of the soil strength plays a role in the design of geotechnical structures, natural slopes and tailing storage facilities.

For many natural soils and tailings a water retention curve (WRC) can be defined mathematically using the fractal characteristics of the particle and pore size distributions. The fractal analogy underpins the mathematical expressions which link degree of saturation (S_r), suction (s) and void ratio (e). For example, key features of the WRC, the air entry suction (s_{ae}) and the air expulsion suction (s_{ex}), are linked to e through power laws in which the power exponent is the fractal dimension of the particle size distribution (Russell [1]).

Here an empirical method is developed that allows estimation of the WRC defining parameters using characteristics of the particles and the pore size distributions. The parameters inside the equations which link s_{ae} and s_{ex} to e, as well as slopes of the curves, may be estimated without resorting to time consuming laboratory testing.

2 Effective stress and water retention in unsaturated soils and tailings

When a soil or tailings is unsaturated a suction s exists and causes the particle contact forces to be larger than what they are when saturated or dry. The suction increases the effective stress and the stiffness of the soil or tailings skeleton. Bishop [2] and Khalili [3] defined this effective stress as

$$\sigma' = \sigma + \chi s \tag{1}$$

where a prime symbol denotes the stress invariant to be effective; σ is the total stress in excess of pore-air pressure (u_a) also referred to as the net stress; s is the difference between pore-air and pore-water pressure ($s = u_a - u_w$); and χ is the effective stress parameter, being 1 for saturated and 0 for dry conditions.

To establish χ it is necessary to consider how water is retained in the soil or tailings. The WRC, i.e. the relationship between S_r and s, is relevant, established usually through experimentation. The WRC may relate s to the gravimetric water content (w) rather than S_r. The relationship between s and S_r (or w) depends on e as well.

For a given e the WRC comprises a main drying curve and a main wetting curve. For a given e and s the S_r on the main drying curve is larger than that on the main wetting curve. When a soil or tailings experiences a change from drying to wetting, or vice versa, the hydraulic state scans between the main drying and wetting curves on what are known as scanning curves. There are an infinite number of scanning curves. A single value of S_r corresponds to an infinite number of possible s values for any given e and the exact value would depend on the mechanical loading and hydraulic history.

* Corresponding author: a.russell@unsw.edu.au

For a given e it is often observed that S_r relates to s in a power law [1, 4]. The main wetting and drying curves and scanning curves are often linear in the double logarithmic S_r versus s plane (Fig. 1). S_r on the main drying and wetting curves may be defined as

$$S_\mathrm{r} = \begin{cases} 1 & \text{for} \quad s \le s_\mathrm{e} \\ \left(\dfrac{s}{s_\mathrm{e}}\right)^{\alpha} & \text{for} \quad s \ge s_\mathrm{e} \end{cases} \tag{2}$$

where α is a negative constant that controls the slopes of the curves. s_e is the s value separating saturated from unsaturated states. For a state on the main drying curve $s_e = s_{ae}$, where s_{ae} is the air entry suction. For a state on the main wetting curve $s_e = s_{ex}$, where s_{ex} is the air expulsion suction. On scanning curves S_r is defined as

$$S_\mathrm{r} = \begin{cases} \left(\dfrac{s_\mathrm{ae}}{s_\mathrm{rd}}\right)^{-\alpha}\left(\dfrac{s_\mathrm{rd}}{s}\right)^{-\beta} & \text{drying} \quad \left(\dfrac{s_\mathrm{ex}}{s_\mathrm{ae}}\right)^{\frac{\alpha}{\alpha-\beta}} s_\mathrm{rd} \le s \le s_\mathrm{rd} \\ \left(\dfrac{s_\mathrm{ex}}{s_\mathrm{rw}}\right)^{-\alpha}\left(\dfrac{s_\mathrm{rw}}{s}\right)^{-\beta} & \text{wetting} \quad s_\mathrm{rw} \le s \le \left(\dfrac{s_\mathrm{ae}}{s_\mathrm{ex}}\right)^{\frac{\alpha}{\alpha-\beta}} s_\mathrm{rw} \end{cases} \tag{3}$$

where β is a negative constant representing the slope of the scanning curves. s_{rd} and s_{rw} represent intercepts of the scanning curves with the main drying and main wetting curves, respectively, and also represent points of suction reversal on the main drying and main wetting curves if suction is suddenly reduced or increased, respectively.

The WRC for a certain e can be made applicable to any other e through s_e. For soils and tailings which have fractal particle size distributions, a theoretical expression for s_{ae} is [1]

$$s_\mathrm{ae} = C_1 e^{-D_\mathrm{s}} \tag{4}$$

in which C_1 is a positive constant with units of stress and D_s is the fractal dimension of the particle size distribution. A constant ratio between s_ae and s_ex is often observed in experiments meaning

$$s_\mathrm{ex} = C_2 s_\mathrm{ae} \tag{5}$$

in which C_2 is a dimensionless constant. The power law dependence of s_e on e has long been observed in experiments as well (e.g. [5]).

For soils and tailings which do not have fractal particle size distributions the relationships between S_r and s, and s_e and e, may have functional forms different from these simple power laws.

Whatever the soil or tailings type, irrespective of whether or not its particle size distribution is fractal, χ may be defined as [6]

$$\chi = \begin{cases} 1 & \text{for} \quad \dfrac{s}{s_\mathrm{e}} \le 1 \\ \left(\dfrac{s}{s_\mathrm{e}}\right)^{\Omega} & \text{for} \quad \dfrac{s}{s_\mathrm{e}} \ge 1 \end{cases} \tag{6}$$

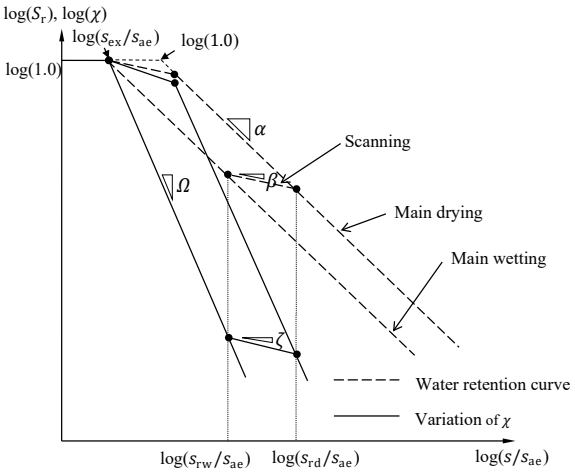

Fig. 1. S_r and χ plotted against s/s_ae in double logarithmic planes.

when the hydraulic state is located on the main wetting or main drying curve. Ω is a negative material constant with a best fit value of -0.55 for a wide range of soil and tailings types. On a scanning curve χ is defined as [7]

$$\chi = \begin{cases} \left(\dfrac{s_\mathrm{rd}}{s_\mathrm{ae}}\right)^{\Omega}\left(\dfrac{s}{s_\mathrm{rd}}\right)^{\zeta} & \text{drying path} \quad \left(\dfrac{s_\mathrm{ex}}{s_\mathrm{ae}}\right)^{\frac{\Omega}{\Omega-\zeta}} s_\mathrm{rd} \le s \le s_\mathrm{rd} \\ \left(\dfrac{s_\mathrm{rw}}{s_\mathrm{ex}}\right)^{\Omega}\left(\dfrac{s}{s_\mathrm{rw}}\right)^{\zeta} & \text{wetting path} \quad s_\mathrm{rw} \le s \le \left(\dfrac{s_\mathrm{ae}}{s_\mathrm{ex}}\right)^{\frac{\Omega}{\Omega-\zeta}} s_\mathrm{rw} \end{cases} \tag{7}$$

where ζ is a negative material constant. The relationship between χ and s is also shown in Fig. 1.

3 Methods

The complete definition of a WRC requires D_s, C_1, C_2, α and β. Of these D_s is the most easily determined. The particle size distribution, when percentage passing is plotted against particle size in a double log plane, forms a straight line and has a slope that is easily measured and equal to $3 - D_s$.

However, the fractal dimension of the pore size distribution (D_p), which relates directly to α through [1]:

$$\alpha = 3 - D_\mathrm{p} \tag{8}$$

is not so easily determined without resorting to time consuming pressure plate tests, filter paper tests, or mercury instruction/extrusion tests, for example. Likewise, parameters C_1, C_2 and β are also not easily determined. They can be quantified, indirectly, using the time-consuming lab testing, although relate to microstructure properties including particle and pore sizes, shapes and surface areas.

Here an empirical technique is used, informed by the underlying fractal theory used to derive Eqs. (4), (5) and (8), to link parameters D_s, C_1, C_2, α and β to particle size properties of the soils and tailings that can be easily determined.

3.1 Experimental program

The WRCs of five tailings considered here were determined as part of the TAILLIQ project (tailliq.com). Some of the WRCs have already been published [8, 9] while others are presented here for the first time. Pressure plate tests and filter paper tests were used. The procedures followed were adapted from ASTM (2016a) and ASTM (2016b), respectively.

3.1.1 Pressure plate

A test involved preparing a number of saturated or near saturated samples at target void ratios, placing the samples on a high air entry pressure plate inside a pressure chamber, pressurising the air in the chamber to target values to induce suction in the samples, enabling pore water to drain from the samples and reach equilibrium, and then measuring the moisture content in the samples. The sample moisture content was then converted to S_r and plotted against s to give the WRC.

Sample preparation differed to that detailed in ASTM (2016a) to obtain samples of different void ratios. Subsequent testing involved increasing suction in increments thus subjecting the samples to a drying process. The volume of each sample was assessed at the end of each suction increment.

A high air entry value porous ceramic plate created a pressure differential between u_w within the plate and an externally applied u_a. For testing the plate was placed in an air tight chamber and a nylon tube was connected from an external graduated burette, through the chamber wall, to a valve on the plate through which the pore water could pass freely. A number of saturated samples were placed on the plate inside the chamber. Chamber air pressure was set to a target value forcing the water from the pores of the soil samples through the plate and nylon tube into the burette. Regular readings of the burette's water level were taken and the vertical position of the burette was adjusted so that the water level remained level with the samples in the chamber. This ensured the pore water pressure in the samples remained constant at zero pressure and equal to the value in the pressure plate. The samples reached states of equilibrium when water ceased to exit the samples, as indicated by a stable water level in the burette. The suction in the samples was easily determined using the relationship $s = u_a - u_w$, where $u_w = 0$.

Each suction increment was applied for a period of around seven days, sufficient for equilibrium to be reached. The chamber air pressure was then quickly reduced to zero. Samples were transferred to moisture content tins, weighed and oven dried at 105^0 C, and their moisture contents determined.

3.1.2 Filter paper test

The test is based on the notion that a filter paper placed in contact with an unsaturated tailings sample will attain the same suction as the sample. The tests involved preparing a number of unsaturated samples at target void ratios, placing a dry filter paper stack (the stack being three pieces of filter paper) in contact with each sample, enabling water to pass from the sample into the filter paper stack and reach equilibrium, and determining the moisture contents of the middle filter paper of the stack and the tailings sample. A calibration curve was then used to estimate the suction in the middle filter paper, from which the suction of the sample was inferred. Sample moisture content is then converted to S_r and plotted against suction and the WRC determined.

Whatman No. 42 filter paper was used as many calibration curves have been published in the literature for it. Samples were prepared in moulds of about 75 mm diameter and 20 mm depth, using light compaction or moist tamping.

For the drying path, samples were initially saturated (or nearly saturated) with distilled water and then allowed to partially dry to a range of moisture contents by placing the samples in an oven for different periods of time. After the desired moisture contents were reached, the samples were then placed in air tight containers for seven days to enable the moisture to distribute evenly throughout the samples.

4 Results

The particle size distributions of five TAILLIQ tailings are shown in Fig. 2 and Fig. 3. The WRCs which have not been previously published are shown in Fig. 4 to Fig. 6, the others can be found in Russell [8] and Vo [9]. The main drying and top scanning curves were fitted using Eqs. (2) and (3). Parameters D_s, α, β, C_1 and $1/C_2$ are listed in Table 1. ζ and Ω are also accounted for by using parameters α and β.

Table 1. Parameters for Gold, Iron Ore, Bauxite, Copper and Platinum tailings that define their WRCs.

	Gold 1	Iron ore	Bauxite	Copper	Platinum
D_s	2.62	2.66	2.84	2.61	2.39
α	-0.65	-0.75	-0.85	-0.24	-0.50
β	-0.18	-0.065	-0.035	-0.042	-0.16
C_1 (kPa)	12	3000	5500	4	64
$1/C_2$	20	1000	5000	8	50

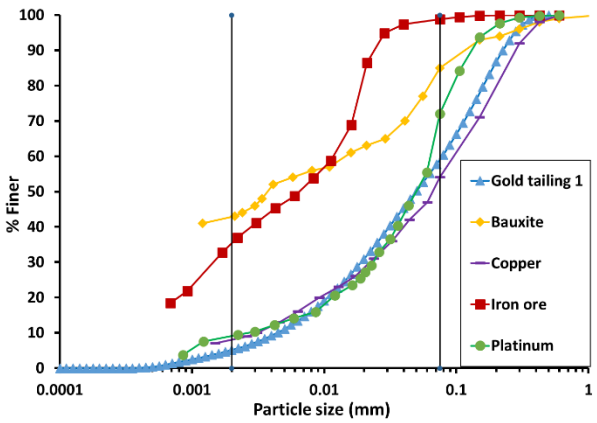

Fig. 2. Particle size distribution of five tailings – traditional presentation.

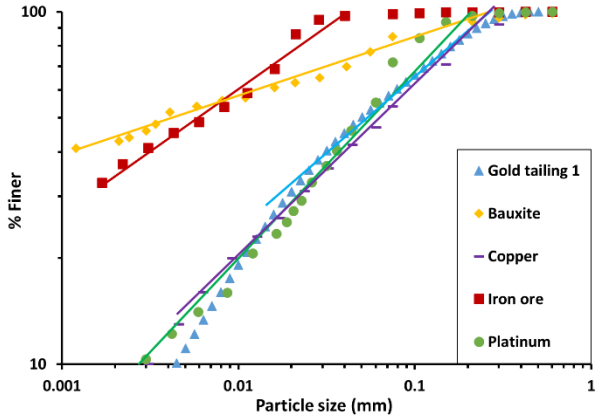

Fig. 3. Particle size distribution of different tailings – double logarithm presentation.

X-ray diffraction analysis for the bauxite tailings shows the presence of phases of gibbsite 43%, boehmite 28%, kaolinite 20%, anatase 3%, hematite 3%, quartz 2% and rutile 1%. And for the iron ore tailings the presence of phases of hematite 44%, kaolinite 34%, muscovite 8%, quartz 8% goethite 4% and clinochlore 2%.

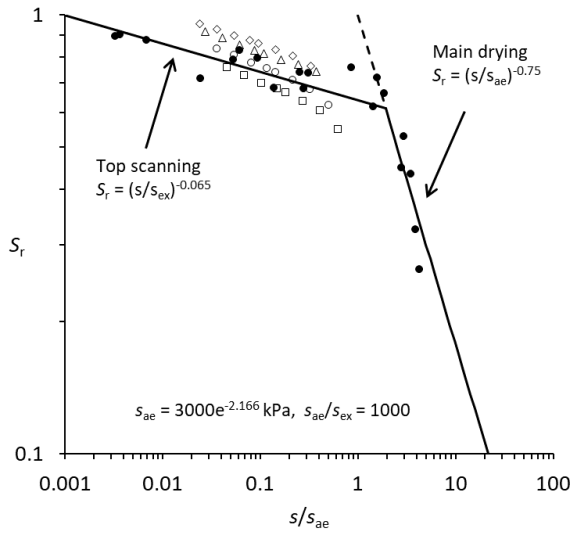

Fig. 4. WRC for the Iron Ore tailings.

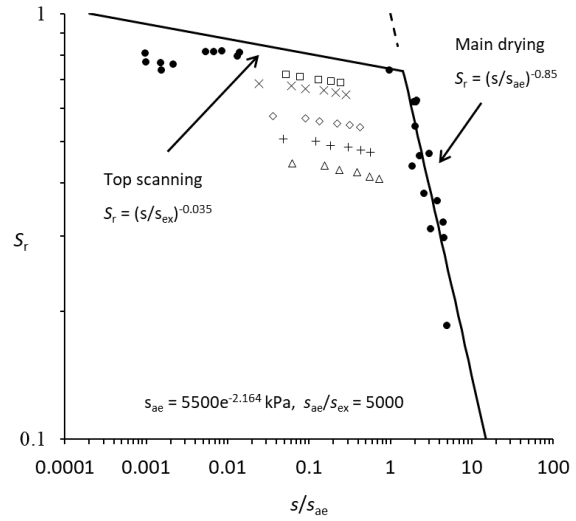

Fig. 5. WRC for the Bauxite tailings.

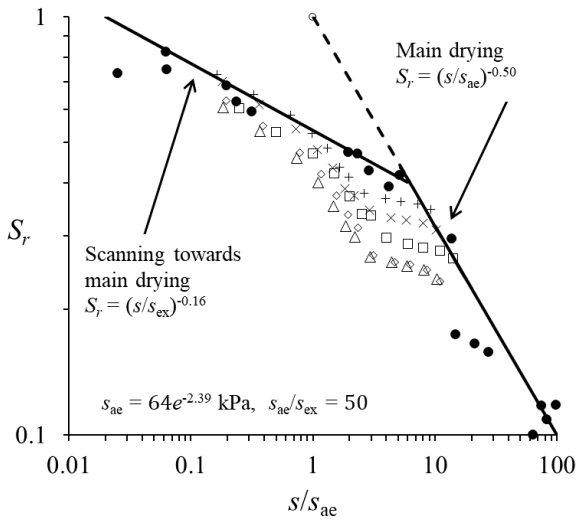

Fig. 6. WRC for Platinum tailings.

Solid symbols represent filter paper test results. Hollow and cross symbols represent pressure plate test results. All test results were obtained by subjecting samples to drying processes.

The particle size distribution and WRCs for two other tailings, and five soils, from the literature are also considered here. Parameters D_s, α, β, C_1 and C_2 for those are listed in Table 2.

Table 2. Parameters for additional five fine-grained soils and two tailings that define their WRCs.

	Lyell silty sand [1]	**Clayey silty sand** [10]	**Silty sand** [11]	
D_s	2.65	2.6	2.55	
α	-0.42	-0.49	-0.65	
β	-0.22	-0.18	-0.06	
C_1 (kPa)	0.8	122	4.5	
$1/C_2$	25	60	3	
	Gold 2 [12]	**Coal** [12]	**London Silt** [13]	**London Clay** [14]
D_s	2.3	2.67	2.15	2.8
α	-0.54	-0.32	-0.715	-0.65
β	-0.174	-0.098	-0.168	-0.063
C_1 (kPa)	16.4	115	10	1200
$1/C_2$	20	50	10	250

5 New empirical correlations

New empirical correlations between the clay percentage and the key parameters of the WRC, including α, β, C_1 and C_2, are provided here.

An empirical expression that relates the clay percentage (by mass) to C_1, as demonstrated in Fig. 7, is:

$$Clay\% = 3.9{C_1}^{0.29} \quad (9)$$

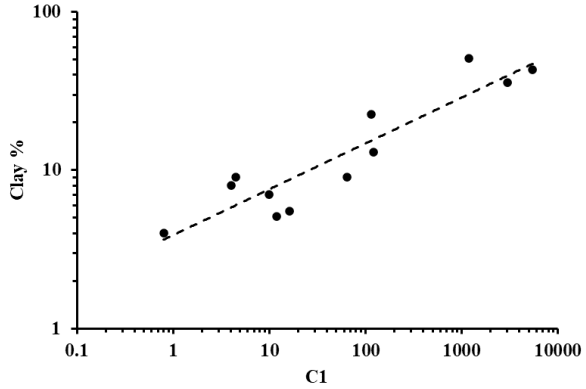

Fig. 7. Clay percentage plotted against $\boldsymbol{C_1}$ in a double logarithmic plane for different soils and tailings.

An empirical expression that relates the clay percentage to C_1C_2, as demonstrated in Fig. 8, is:

$$Clay\% = 9.1C_1C_2 \quad (9)$$

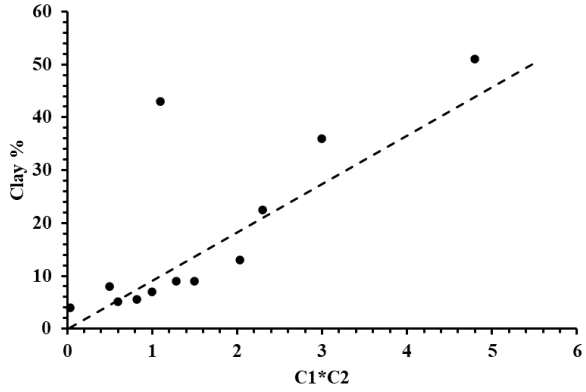

Fig. 8. Clay percentage plotted against $\boldsymbol{C_1C_2}$ for different soils and tailings.

In order to estimate α using the clay percentage a new coefficient C_3 is introduced. It is related to the s value when S_r = 10% through:

$$s_{10} = C_3 e^{-D_s} \quad (10)$$

An interrelationship between C_3, C_1 and α then exists and is of the form:

$$0.1 = (C_3/C_1)^{-\alpha} \quad (11)$$

The empirical expression that relates the clay percentage to C_3 in Fig. 9 is:

$$Clay\% = {C_3}^{0.32} \quad (12)$$

Combining Eqs. 13 and 14 enables α to be determined. In Fig. 10 the clay percentage is related to β through:

$$Clay\% = -260\,\beta + 55 \quad (13)$$

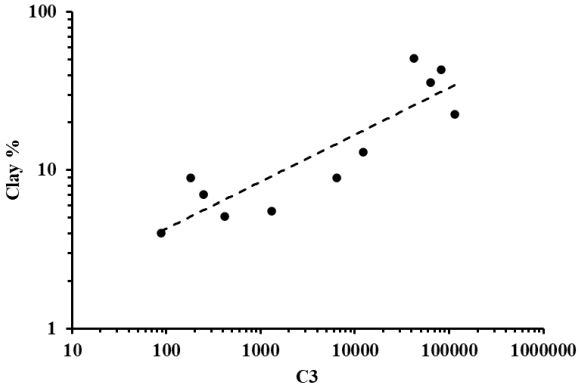

Fig. 9. Clay percentage plotted against $\boldsymbol{C_3}$ in a double logarithmic plane for different soils and tailings.

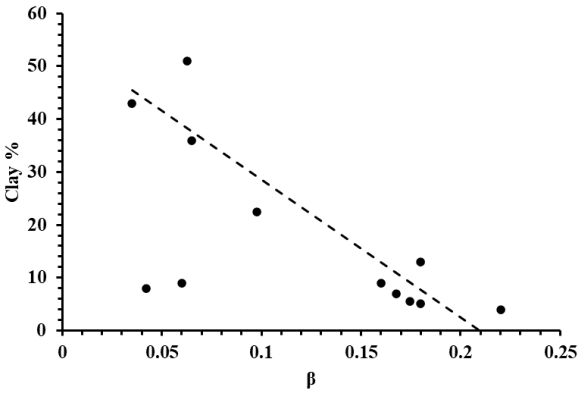

Fig. 10. Clay percentage plotted against $\boldsymbol{\beta}$ for different soils and tailings.

6 Demonstration of accuracy

Empirical predictions of the WRCs using Eqs. 4, 5, 9-14 are compared with a selection of the WRCs that were fitted directly to the laboratory data. These are shown in Figs. 11 to 14. Continuous lines represent WRCs from the laboratory and dashed lines represent the estimated WRCs. Reasonable agreement is shown.

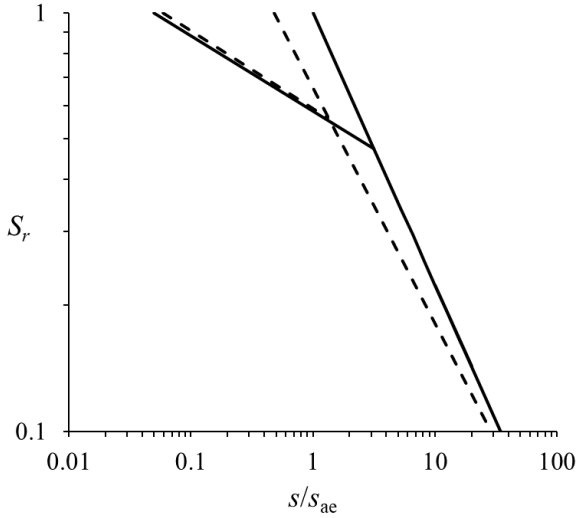

Fig. 11. WRCs for Gold tailings 1.

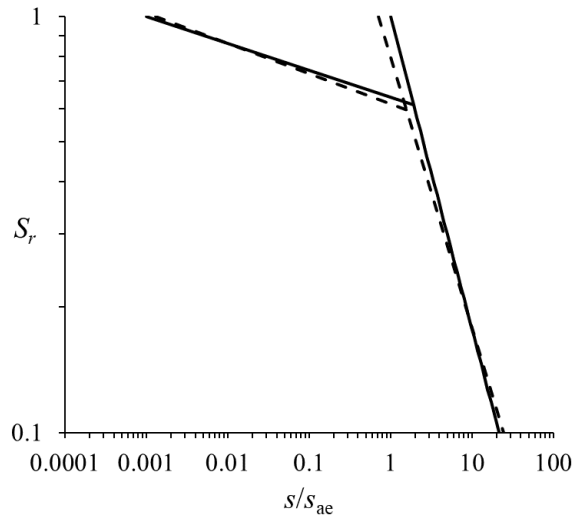

Fig. 12. WRCs for Iron ore tailings.

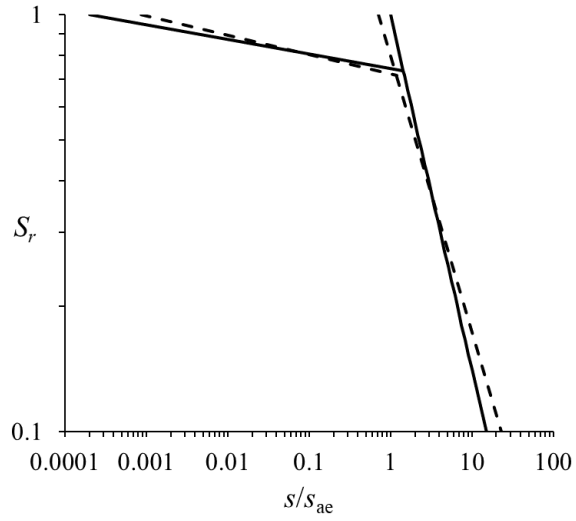

Fig. 13. WRCs for Bauxite tailings.

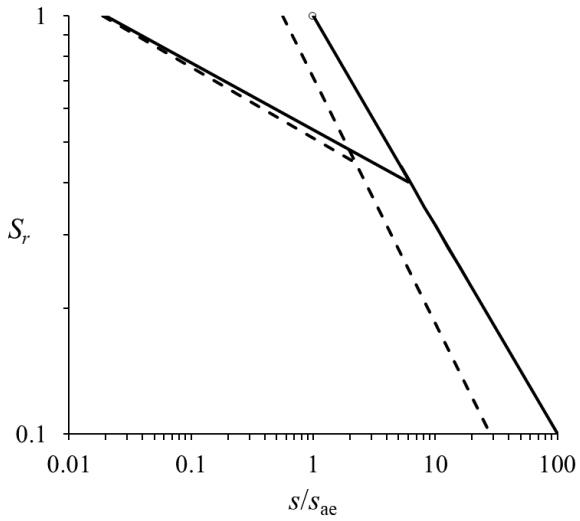

Fig. 14. WRCs for Platinum tailings.

Blind predictions would provide further evidence of the accuracy of this approach and would be a welcome focus of future research.

7 Conclusion

This work demonstrates how the key defining parameters of a fractal WRC may be related to easily measured particle size information through empirical expressions, avoiding the need for time consuming laboratory testing. A variety of fine-grained soils and tailings were used. Once the WRC is known the effective stress parameter may be determined, enabling suction's contribution to strength to be estimated for a given moisture content, adding to the practical appeal of this work.

Part of this work stems from TAILLIQ (Tailings Liquefaction), which is an Australian Research Council (ARC) Linkage Project (LP160101561) supported by financial and in-kind contributions from Anglo American, BHP, Freeport-McMoRan, Newmont, Rio Tinto and Teck. The TAILLIQ project is being carried out at The University of New South Wales, The University of South Australia, The University of Western Australia (lead organisation) and The University of Wollongong. We acknowledge the support and contributions of project personnel at each of the supporting organisations. The work also forms part of an ARC Future Fellowship (FT200100820) awarded to the corresponding author and that funding is gratefully acknowledged.

References

1. A.R. Russell, Géotechnique, **64**, 5 (2014)
2. A.W. Bishop, Tek. Ukebl., **106**, 39 (1959).
3. N. Khalili, F. Geiser, G.E. Blight, Int. J. Geomech., **4**, 2 (2004)
4. R. Brooks, A. Corey, Hydrol. Pap. Color. State Univ., **3**, March (1964)
5. G.E. Laliberte, A.T. Corey, R.H. Brooks, Hydrol. Pap., **17** (1966)
6. N. Khalili, M.H. Khabbaz, Géotechnique, **48**, 5 (1998)
7. N. Khalili, S. Zargarbashi, Géotechnique, **60**, 9 (2010)
8. A.R. Russell, T. Vo, J. Ayala, Y. Wang, D. Reid, A.B. Fourie, Géotechnique, 10.1680/jgeot.21.00261, (2022)
9. T. Vo, Y. Wang, A.R. Russell, Géotechnique, **72**, 3 (2022)
10. S. Salager, M.S. El Youssoufi, C. Saix, Can. Geotech. J., **47**, 6 (2010)
11. S. Huang, S.L. Barbour, D.G. Fredlund, Can. Geotech. J., **35**, 3 (1998)
12. Y. Qiu, D.C. Sego, Can. Geotech. J., **38**, 1 (2001)
13. P. MacKay, "Evaluation of Oxygen Diffusion in Unsaturated Soils," (1997).
14. X. Zhang, M. Mavroulidou, M.J. Gunn, *E3S Web Conf.*, **vol. 9**, (2016)